Structure Design and Fabrication of Symmetric Force-balance Micromachining Capacitive Accelerometer

Qiang Zou ; Deren Lu ; Baoqing Li ; Xingguo Xiong ; Bin Xiong; Weiyuan Wang

State Key Lab of Transducer Technology, Shanghai Institute of Metallurgy, Chinese Academy of Sciences, 865 Changning Road, Shanghai 200050, P.R. China

Qiang Zou ; Deren Lu ; Baoqing Li ; Xingguo Xiong ; Bin Xiong, et al. "Structure design and fabrication of symmetric force-balance micromachining capacitive accelerometer", Proc. SPIE 3223, Micromachining and Microfabrication Process Technology III, 284 (September 5, 1997); doi:10.1117/12.284492

PROCEEDINGS OF SPIE
SPIE—The International Society for Optical Engineering

Micromachining and Microfabrication Process Technology III

Shih-Chia Chang
Stella W. Pang
Chairs/Editors

29–30 September 1997
Austin, Texas

Sponsored by
SPIE—The International Society for Optical Engineering
SEMI—Semiconductor Equipment and Materials International
NIST—National Institute of Standards and Technology

Cooperating Organization
Solid State Technology

Published by
SPIE—The International Society for Optical Engineering

Volume 3223

Structure Design and Fabrication of Symmetric Force-balance Micromachining Capacitive Accelerometer

Qiang Zou Deren Lu Baoqing Li Xingguo Xiong
Bin Xiong Weiyuan Wang

State Key Lab. of Transducer Technology, Shanghai Institute of Metallurgy,
Chinese Academy of Sciences, 865 Changning Road, Shanghai 200050, P.R.China

ABSTRACT

A novel KOH silicon maskless anisotropic etching technology is adopted to fabricate micromachining silicon mass-beam structure accelerometer. Lateral sensitivity effect in normal accelerometer is eliminated because the beams which are thinner than 15μm have been formed in the middle of the seismic mass. Based on the calculation of sensitivity and basic resonance frequency of two kinds of bulk micromachining accelerometers, the structure parameters of cantilever and double-side-supported accelerometer have been optimized by using the sensitivity -frequency product as the figure of merit of a structure. The different etching characteristics of {311} and {100} plane of silicon in KOH maskless anisotropic etching process have been investigated thoroughly and utilized in the fabrication of symmetric mass-beam structure. Special damping design has been proposed to reduce the damping ratio of the device in order to improve the dynamic performance of the accelerometer. Preliminary measurement of the static characteristics of the structure has been performed with a force-deflection balance measurement apparatus.

Key Words: micromachining, maskless anisotropic etching, accelerometer

INTRODUCTION

Micromachining silicon accelerometers are becoming more and more important for a wide range of applications, including the aerospace, automotive, medical and mechanical industry fields. Many kinds of Piezoresistive [1-3] and capacitive[4-6] micromachining accelerometers have been developed and some have already been in commercial production[7]. Because the force-balance micromachining accelerometer has excellent performance such as high precision, excellent linearity and excellent stability, it stimulate the most intense interest among the researchers. Normally the detection principle of the force-balance micromachining accelerometer is capacitive because the capacitive electrode can provide electrostatic force to make the movable mass back to the balance position. Now we fabricated out the symmetric capacitive force-balance accelerometer by bulk micromachining technology, which can overcome the process complexity of surface micromachining accelerometer and can be produced at lower price. In the normal mass-beam structure accelerometers, the supported beams are located at the top or the bottom of the wafer. This configuration will lead to a serious problem —lateral sensitivity effect. Because the beams are not in the same plane of the centroid of the mass, acceleration along the beam direction can also cause the mass to move from the equilibrium position. If the beams can be formed in the middle of the mass, lateral sensitivity effect of the accelerometer can be eliminated because the beams are in the same plane as the one which includes the mass centroid. Based on this principle, one approach is presented to suspend the mass from top and bottom of the wafer. This double suspension scheme requires more manufacturing steps such as highly doping[8] or different suspension materials[9]. Now we adopted the maskless anisotropic etching technology to make out beam-mass structure accelerometer whose beams are formed in the middle of the mass. After glass-silicon anodic bonding , the glass-silicon-glass "sandwich"structure differencial capacitive accelerometer can be made out. The diagram of the accelerometer structure is shown in Fig.1. Movable mass is employed to sense the acceleration. At the same time, it is differential capacitor's movable electrode. The stationary electrode is made from aluminium which is deposited and patterned on the glass.

SPIE Vol. 3223 • 0277-786X/97/$10.00

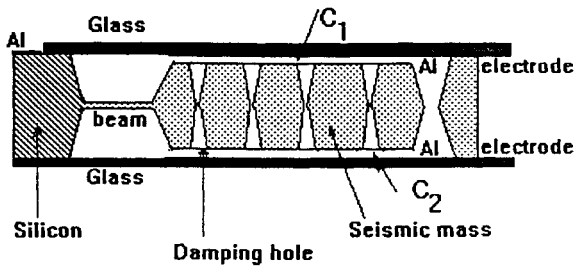

Fig.1 Diagram of the cantilever structure symmetric capacitive accelerometer

STRUCTURE DESIGN

1. Basic Structure Parameters

In the design of accelerometer structure, two characteristics should be considered—sensitivity and resonant frequency. Sensitivity determines the output characteristics of the device. We hope sensitivity of the device is as higher as possible. Accelerometer is a dynamic device. When there is an alternative acceleration, the mass-beam system will vibrate. So the frequency bandwidth of the accelerometer is a very important characteristics of the device. When there is no damping, the frequency bandwidth of the device is determined by the resonance frequency of the structure. When sensitivity of the device rises, its resonant frequency goes down, or vice versa. We hope the accelerometer has higher sensitivity and at the same time it should have enough frequency bandwidth, otherwise it has no practical use. So we adopt the sensitivity-frequency product as the figure of merit of a structure in order to optimize the structure parameters of the device[10]. Double parallel straight beams were employed to replace the single beam in order to improve lateral rigidity of the structure. Then this structure is less sensitive to cross acceleration. The special "peninsula"structure is added to the seismic mass to increase the mass and capacitive value of the accelerometer.

1.1 Mechanical Analysis

1) Cantilever structure

Figure 2 shows the dimensions and force conditions of the cantilever mass-beam structure when acceleration with value a is applied to it. Based on the principal of the Elastic Mechanics, moment equations can be written as the following:

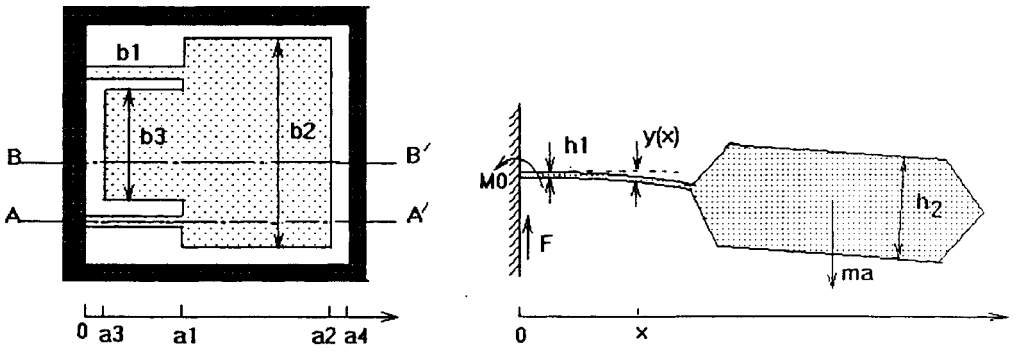

(a) top view (b) side view

Fig2. Diagram of cantilever beam-mass structure

$$EI_1 y''(x) = M_0 - Fx \qquad (0 \le x \le a_1) \qquad (1)$$

$$EI_2 y''(x) = M_0 - Fx + \rho \cdot b_3 \cdot (a_1 - a_3) \cdot h_2 \cdot a \cdot (x - \frac{a_1 + a_3}{2}) + \frac{1}{2} \cdot \rho \cdot a \cdot b_2 \cdot h_2 \cdot (x - a_1)^2 \qquad (a_1 \le x \le a_2) \qquad (2)$$

Here , $F = m \cdot a$

$$M_0 = m \cdot a \cdot a_2 - \rho \cdot b_3 \cdot (a_1 - a_3) \cdot h_2 \cdot a \cdot (a_2 - \frac{a_1 + a_3}{2}) - \frac{1}{2} \cdot \rho \cdot a \cdot b_2 \cdot h_2 \cdot (a_2 - a_1)^2$$

E is the Young's modulus, I_1 and I_2 is the inertia mudulus of beam and mass respectively, and the meanings of the other letters are shown in Fig.2. While the boundary conditions are

$$\begin{cases} y/_{x=0} = 0 \\ y'/_{x=0} = 0 \\ y''/_{x=a_2} = 0 \end{cases} \tag{3}$$

On the assumption that there is no elastic deformation on the mass, then we can get the displacement of each part of the mass-beam structure :

$$y(x) = \frac{1}{EI_1} \cdot (\frac{1}{2} \cdot M_0 \cdot x^2 - \frac{1}{6} \cdot F \cdot x^3) \qquad (0 \le x \le a_1) \tag{4}$$

$$y(x) = y(x)/_{x=a_1} + y'/_{x=a_1} (x - a_1) = \frac{1}{E \cdot I_1} \cdot (\frac{1}{2} \cdot M_0 \cdot a_1^2 - \frac{1}{6} \cdot F \cdot a_1^3) + \frac{1}{E \cdot I_1} (M_0 \cdot a_1 - \frac{1}{2} \cdot F \cdot a_1^2) \cdot (x - a_1) \qquad (a_3 \le x \le a_2) \tag{5}$$

2) Double-side-supported structure

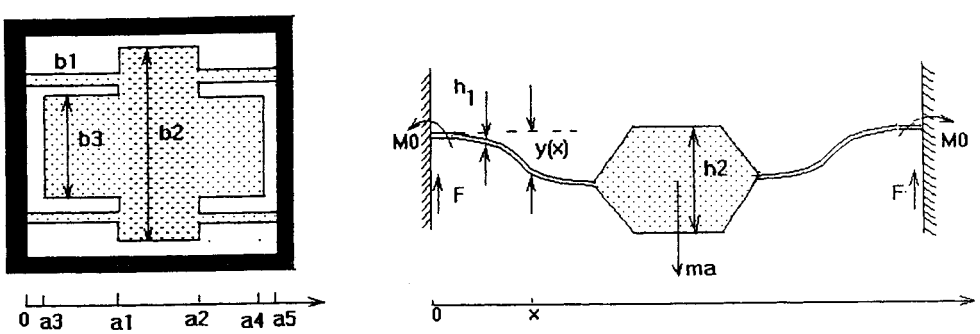

(a) top view (b) side view

Fig3. Diagram of double-side-supported mass-beam structure

Figure 3 shows the dimensions and force conditions of the double-side-supported mass-beam structure when acceleration with value a is applied to it. Based on the principal of the Elastic Mechanics, moment equations can be written as the following:

$$EI_1 y''(x) = M_0 - F \cdot x \qquad (0 \le x \le a_1) \tag{6}$$

$$EI_2 y''(x) = M_0 - Fx + \rho \cdot b_3 \cdot (a_1 - a_3) \cdot h_2 \cdot a \cdot (x - \frac{a_1 + a_3}{2}) + \frac{1}{2} \cdot \rho \cdot a \cdot b_2 \cdot h_2 \cdot (x - a_1)^2 \qquad (a_1 \le x \le a_2) \tag{7}$$

$$EI_3 y''(x) = M_0 - Fx + M \cdot a \cdot (x - \frac{a_3 + a_4}{2}) \qquad (a_2 \le x \le a_5) \tag{8}$$

While the boundary conditions are

$$\begin{cases} y/_{x=0} = y'/_{x=0} = 0 \\ y/_{x=a_5} = y'/_{x=a_5} = 0 \\ y''/_{x=\frac{a_1}{2}} = 0 \end{cases} \tag{9}$$

Because the elastic deformation can be neglected, each point on the mass has the same displacement when the frame of the structure accelerates. The displacement of every part of this mass-beam structure can be described as following:

$$y(x)=\frac{1}{E\cdot I_1}\cdot(\frac{1}{2}\cdot M_0\cdot x^2-\frac{1}{6}\cdot F\cdot x^3) \qquad (0\le x\le a_1) \tag{10}$$

$$y(x)=\frac{1}{E\cdot I_1}\cdot(\frac{1}{2}\cdot M_0\cdot a_1^2-\frac{1}{6}\cdot F\cdot a_1^3) \qquad (a_1\le x\le a_2) \tag{11}$$

$$y(x)=\frac{1}{E\cdot I_3}\cdot(\frac{1}{2}\cdot M_0\cdot x^2-\frac{1}{6}\cdot F\cdot x^3+m\cdot a\cdot(\frac{1}{6}\cdot x^3-\frac{a_3+a_4}{4}\cdot x^2))+\frac{1}{EI_3}\cdot(\frac{1}{2}\cdot F\cdot(a_3+a_4)^2-M_0\cdot(a_3+a_4))\cdot x+\frac{1}{EI_3}(\frac{1}{2}\cdot M_0\cdot(a_3+a_4)^2-\frac{1}{12}\cdot m\cdot a\cdot(a_3+a_4)^3) \tag{12}$$

$$(a_2\le x\le a_5)$$

Where $F=\frac{1}{2}\cdot m\cdot a$, $M_0=\frac{1}{4}\cdot m\cdot a\cdot a_1$

1.2 Sensitivity analysis

If there is no acceleration, mass is at the balance position. At this situation, the up-capacitor C_1 and down-capacitor C_2 in this device are same:

$$C_1=C_2=\frac{\varepsilon_0\cdot\varepsilon\cdot A}{d_0} \tag{13}$$

When an acceleration perpendicular to the beam plane is applied to the structure, the beams deform and so the mass deviates from the balance position. The displacement of every point of the mass can be described as y(x), then the up and down capacitor of this capacitive accelerometer can be described as:

$$C_1=\int_{a_1}^{a_2}\frac{\varepsilon_0 cb_2}{d_0-y(x)}dx+\int_{a_3}^{a_1}\frac{\varepsilon_0 cb_3}{d_0-y(x)}dx \tag{14}$$

$$C_2=\int_{a_1}^{a_2}\frac{\varepsilon_0 cb_2}{d_0+y(x)}dx+\int_{a_3}^{a_1}\frac{\varepsilon_0 cb_3}{d_0+y(x)}dx \tag{15}$$

The sensitivity of the accelerometer can be represented as:

$$S=\frac{\Delta C}{\Delta a}=\frac{C_2-C_1}{\Delta a} \tag{16}$$

In order to optimize the structure parameters, the fabrication process characteristics should be considered at the same time.Some parameters must be defined previously. The area occupied by the whole mass-beam structure is 4000μm×4000μm. Because the characteristics of anisotropic etching, the included angle about 54.7°is formed between {111}plane and {100}plane of silicon. In order to etch through the wafer and leave enough area to arrange the corner compensation patterns, the distance between the edge of mass and the edge of the structure frame must be large enough. We define this distance as 400μm. So the width of the mass is 3200μm. We define the width of the beam as 150μm, but its width on mask is much larger than this ,which is controlled by characteristics of maskless anisotropic etching and will be discussed in detail in the following section. The width of the peninsula is 1320μm, so the space for corner compensation and through etching is left. The smaller the capacitive distance, the more sensitive of the capacitive accelerometer. But smaller capacitive distance will be hard realized in the fabrication process. We define the capacitive distance 4μm as the one usually accepted. The thickness of the mass is determinated by the thickness of wafer, it is about 300μm. Based on the results and parameters mentioned above, the sensitivity as the function of beam length and thickness can be caculated.

Figure 4 and 5 show the sensitivity as function of beam high and beam length respectively. With the increase of beam high, the sensitivity of both cantilever and double-side-supported structure goes down. With the increase of beam length, the sensitivity of cantilever structure goes up at first and then goes down. When the beam length is 1500μm, the sensitivity of this structure reaches its maxium value. However with the increase of beam length, the sensitivity of double-side-supported structure increase continuously. It is obvious that the sensitivity of cantilerver structure is much higher than that of the double-side-supported structure. For instance, when beam length is 1400μm and beam high is 20μm, the sensitivity of cantilever is 58.1PF/g, while the sensitivity of double-side-supported structure is only 1.1PF/g.

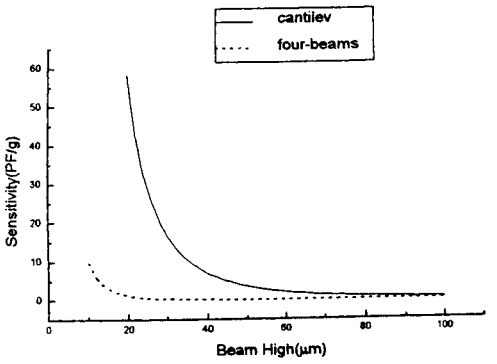

Fig.4 Sensitivity as the function of beam high

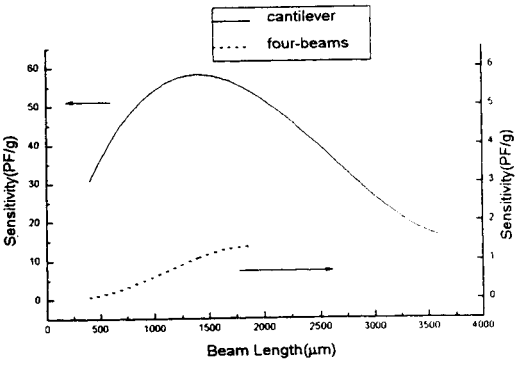

Fig.5 Sensitivity as the function of beam length

1.3 Frequency analysis

The basic model of the mass-beam structure is mass-spring system.According to the vibratory theory,we adopt the Reily-Ritz method to caculate the resonant frequency of the structure[11]:

$$\omega^2 = \frac{\int EI(\frac{d^2y}{dx^2})^2 dx}{\int \rho A y^2(x) dx} \tag{17}$$

The caculated results of resonant frequency of cantilever and double-side-supported structure as the function of beam high and beam length are shown in Fig.6 and 7 respectively. We find that with the increase of beam high, the frequency of both cantilever structure and double-side-supported structure increase. With increase of beam length, the frequency of doule-side-supported structure decreases, However, the frequency of cantilever structure decrease firstly then increase after its minimum value when its length is 1900μm due to the total mass decreases. Generally, the frequency of double-side-supported structure is much higher than that of the cantilever structure. For instance, for the structures with 20μm beam high and 500μm beam length, the frequency of cantilever structure is 247.5Hz. while the frequency of double-side-supported structure is 3463 Hz.,which is about one order higher than that of the cantilever structure.

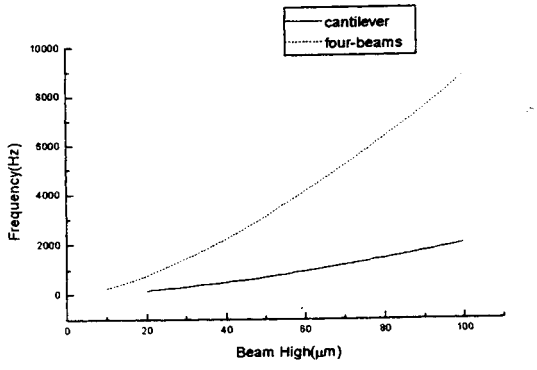

Fig.6 Frequency as the function of beam high

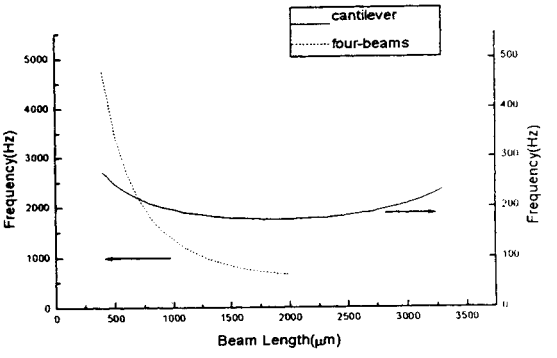

Fig.7 Frequency as the function of beam length

The frequency -sensitivity product as the function of beam high and beam length in cantilever structure are shown in Fig.8 and 9 respectively. It can be seen that the optimized beam length of cantilever structure is between 1100μm~1400μm. We also find that the thinner the beam,the higher the frequency-sensitivity product. That is to say, the thinner the beam, the better performance of the accelerometer. But the thinner beams are very easily broken during the fabrication process. In order to get high yield, the beam high are normally controlled between 10μm~20μm.

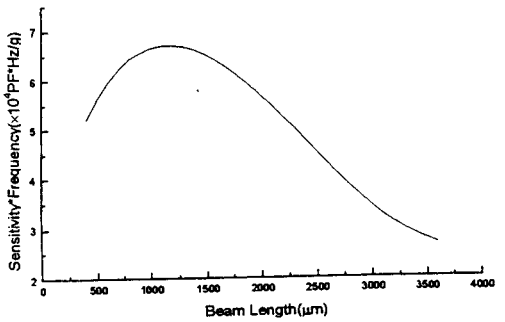

Fig.8 Sensitivity-Frequency product as the function of beam length

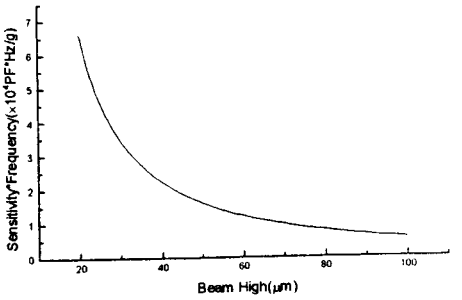

Fig.9 Sensitivity-Frequency product as the function of beam high

2.Damping

Squeeze air film damping is a fudamental fact to determinate the dynamic characteristics of the accelerometer. For the force-balance capacitive accelerometer, the displacement of mass is very small. So the squeeze air film can satisfy the conditions of the isothermal, small-pressure-variation and small displacement assumption.Under this condition,the Navier-stokes equation which govern the behavior of air fluid can be simplified as[12]:

$$\frac{\partial^2 p}{\partial x^2}+\frac{\partial^2 P}{\partial y^2}=\frac{12\mu}{h^3}(\frac{dh}{dt}) \tag{18}$$

The capacitive accelerometer can be modeled as rectangular shape mass-beam system which vibrate in the squeeze air fluid.When rectangular boundary conditions are applied to the above equation, the accelerometer damping ratio ξ can be represented as:

$$\xi=\frac{\beta(\frac{W}{L})W^2\mu}{t\times\rho\times h^3\times 2\omega_0} \tag{19}$$

Where,W and L is the equivalent width and length of the mass respectively, μ is the coefficient of viscosity of air, t is the mass thickness, ρ is the density of mass, h is the capacitive distance and ω_0 is the rensonant frequency of the device. If ξ has the optimized value 0.707, the largest stable work frequency bandwidth of the accelerometer can be achieved. Applied the basic structure parameters to the above formula , we get ξ=270 >>0.707. In order to lower down the damping ratio ξ, an effective method is to make many holes on the mass. The damping holes divide the whole mass into many smaller mass. The length of every smaller mass is 1/N of the one of the big mass. Because $\xi \propto W^2$, so the damping ratio of smaller mass is reduced to $1/N^2$ of the damping ratio of big mass. By adjusting the quantity and dimension of the smaller mass, the damping ratio of the device can be reduced effectively. For the practical fabricated structure in this work, damping ratio of the accelerometer can be reduced to less than 0.9.

FABRICATION PROCESS

The fabrication process for the bulk micromachining accelerometer was developed by KOH anisotropic etching technology which is convenient for industrial application because of its good uniformity in etch characteristics and it is cheaper than dry etching process. In order to make the beams to place in the middle of the mass, we adopt the method to photolithograph and etch from both sides of the wafer. Fig.10 shows the fabrication process of the bulk micromachining accelerameter. A-A' and B-B' are the cross section of the cantilever structure as shown in Fig.2(a) .

1.Fabrication Process Sequence

1.First oxidation

2.First oxide patterning

3.First etching

4.Second oxidation

5.Second oxide patterning

6.Second etching

7.Third oxide patterning

8.Third etching

9.Laser cutting

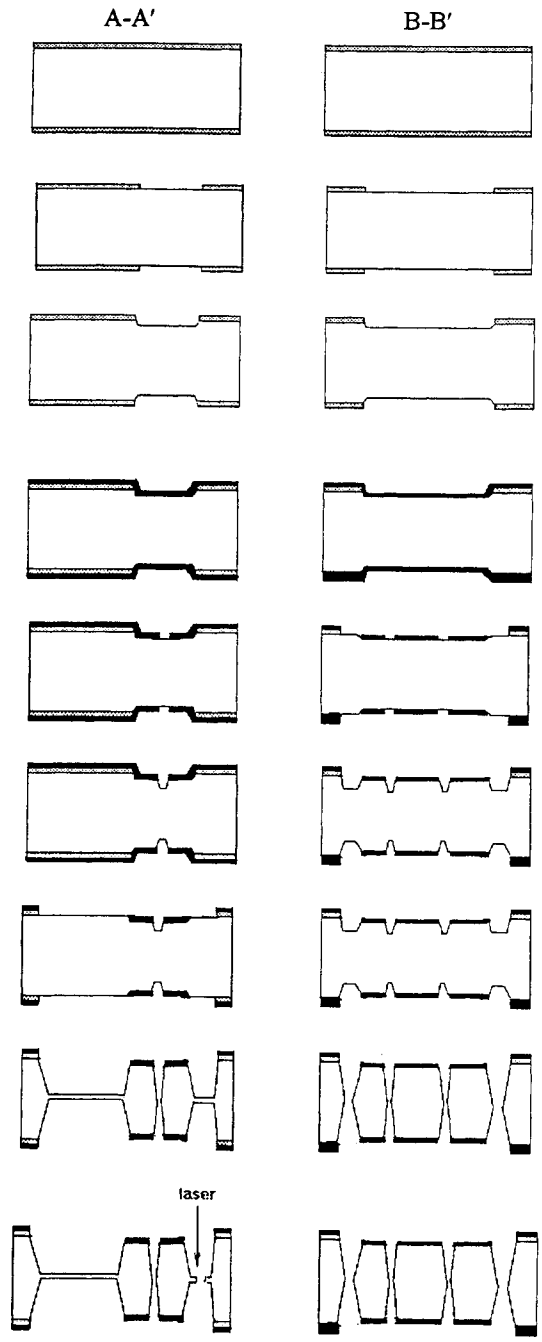

Fig.10 Fabrication Process Sequence

Each step of the following process is performed from both sides of the wafer at the same time.The starting materials is ϕ50, both sides polished, 300μm thickness, (100)orientation silicon wafer with $10\,\Omega \cdot cm$ resistivity. The time of first oxidation is shorter, thermally growing SiO_2 about 0.1μm. The following step is first oxide patterning, which defines the rectangular shape "etching window". The aim of first etching step is to define the capacitor distance 4μm, which is very important for the sensitivity and damping characteristics of the accelerometer device. The next step is second oxidation, thermally growing SiO_2 greater than 1μm, which act as the mask to prevent mass from long time KOH etching. Second oxide patterning are carried out to define the groove area which will be etched through in the future. At the same time, damping holes also are defined. Then second etching can be performed, in which the etching depth is equal to the half of the desired thickness of beams. At this time, the surface of the "beam body" and the surface of wafer are at the same level. Then the third oxide patterning is performed to get rid of the SiO_2 of the "beam body". At this stage, there is no SiO_2 on the surface of "beam body" and the bottom of groove on the both sides of the wafer. Then the maskless anisotropic etching is carried out. That is to say, the "beam body"and the bottom of groove are etched at the same time from both sides of the wafer. Because the surface of "beam body"is higher than the bottom of groove, which maintains the half of desired thickness of the beam throughout the etching process. So as the grooves are just etched through, the beam body is reduced to the expected thickness and placed to the middle of the mass.

We have already fabricated out the bulk micromachining symmetric capacitive accelerometer by the maskless anisotropic etching technology.The chip SEM photographs are shown in Fig.11.

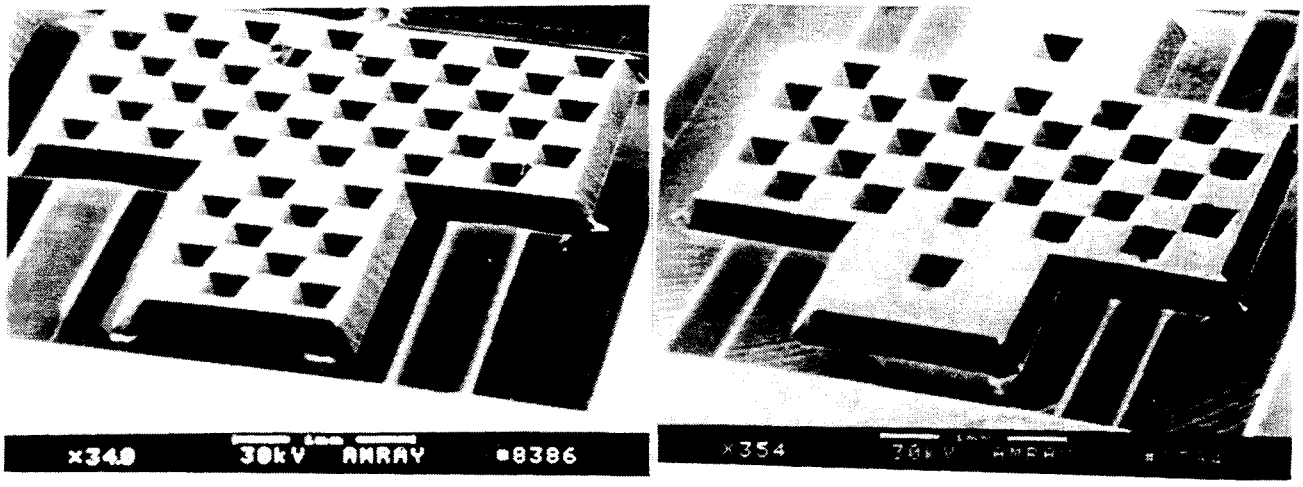

(a)Cantilever structure (b)Double-Side-Supported Structure

Fig.11 SEM Photograph of Accelerometer Chip

2.Maskless anisotropic etching technology

In order to make out the symmetric beam-mass structure, maskless anisotropic etching technology is adopted.The process of maskless anisotropic etching can be described with Fig.12.

Before the maskless anisotropic etching, there is a mesa constructed by the surface of the "beam body" and the bottom of the groove. Both of them are (100) plane. The high of the mesa is the half of desired thickness of the beam. When SiO_2 on the "beam body"is stripped away, both the plane (100) of beam body and that of groove bottom are etched in the KOH solution with same etching rate at the same time. There appears a new fast etching plane along the mesa's edges. This new plane extends continuously in the etching process . After it replaces all (111)plane, it continues to move down along the groove bottom. Before the through etching of the wafer finishes, measurement shows that the angle between this plane and (100) plane is 23.8°. It is proved that this new plane is (311), concording with the previous report[13]. Because of the edge recession during the maskless etching process, the final beam width is much smaller than the beam width at the etching beginning. The relationship between the final beam's width and the beam width of mask can be written as the following equation:

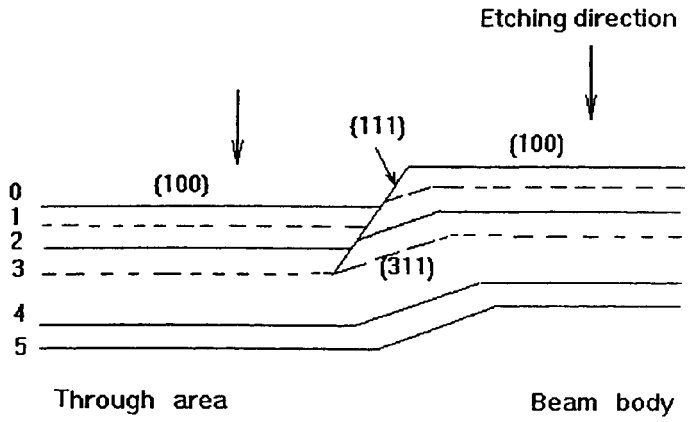

Fig.12 Process of maskless anisotropic etching

$$B = b + (2.3486 \times r - 2.1251) \times (D - d) \tag{20}$$

Where, B and b is the beam width on the mask and final beam width respectively. r is the etching ratio between (311) and (100) of silicon, its value is 1.61 in our experiment. D and d is the thickness of wafer and the desired thickness of final beam respectively. But after through etching finishes, the side plane of the beam is no longer consist of the single (311) plane. This situation maybe begin from the time at which the {111} side plane of the mesa just disappears, however, the relationship of equation (20) is proved correct in experiment.

PRELIMINARY MEASUREMENT

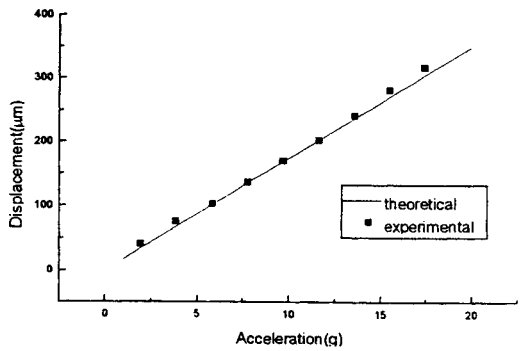

Fig.13 Static performance of Cantilever structure accelerometer

We adopt the balance-approach to investigate the static performance of cantilever structure accelerometer which is shown in Fig.2[14].The theoretical and measured static performance of the cantilever mass-beam structure are in accordance with each other very well, as shown in Fig.13. Sensitivity of centroid displacement of this mass-beam structure can be achieved as 17.95μm/g, which is consistent well with the caculated result 17.48μm/g based on the theory mentioned above.

CONCLUSION

Two kinds of bulk micromachining symmetric structures designed for force-balance capacitive accelerometer were presented. The mechanical, sensitivity, frequency analysis and the damping design were carried out. The sensitivity of the both structures decrease fast with increase of the beam high, while changes differently with the beam length. For double-

side-supported structure the sensitivity increases slowly with increase of the beam length. But for the cantilever structure the sensitivity goes up first and then goes down. The maxium sensitivity happens at about 1500μm for the cantilever structure with the parameters proposed in this work. The frequency analysis shows that the resonant frequency increases with the beam high, while decreases with the beam length for the double-side-supported structure and decreases slowly first then increases a little if the beam length increases for the cantilever structure. The damping analysis shows that making many damping holes on the seismic mass, a desired damping ratio can be achieved. The fabrication process including a maskless anisotropic etching was described. In the maskless anisotropic etching, a new side plane {311} replace the original {111} side plane of the beam. The static sensitivity of the fabricated structures were measured using a force-deflection balance measurement apparatus. The measured static sensitivities were consistent well with the analysis in this paper.

ACKNOWLEDGEMENT

This work was supported by National Climbing Program-B on "Micro ElectroMechanical System",China.

REFERENCES

1.Lynn Michelle Roylance, et al, A Batch-Fabrication Silicon Accelerometer, IEEE Trans. on Electron Devices, Vol. ED-26,pp.1911,(1979).
2.H.Sandweier, et al,A Silicon Based Micromechanical Accelerometer with Cross Acceleration Sensitivity Compensation, *Transducer'87*,pp.399-402,(1987)
3.J.T.Suminto , et al, A Simple High Performance Piezoresistive Accelerometer, *Proc. 6th Int. Conf.Solid-state Sensor and Actuator(Transducer'91)*, pp.104-107, San Francisco, CA,USA, (1991)
4.S.Suzuki, et al, Semiconductor Capacitive-type Accelerometer with PWM Electrostatic Servo Technique, *Proc. of the SAE'91*, Detroit,USA, (1991)
5.J.Cole, A New Sense Element Technology for Accelerometer Subsystems, *Proc. 6th Int. Conf.Solid-state Sensor and Actuator(Transducer'91)*, pp.93-96, San Francisco, CA,USA, (1991)
6.F.Rudolf, et al , Precision Accelerometers with μg Resolution, Sensors and Actuators, A21-23, pp.297-302, (1990)
7.Wolfgang Kuehnel, et al, A surface Micromachied Silicon Accelerometer with on-chip Detection Circuitry , Sensors and Actuators , A45(1994), pp.7-16(1994)
8.H.Seidel, et al , Capacitive Silicon Accelerometer with Highly Symmetrical Design, Sensors and Actuators, A21-23, pp.312-315,(1990)
9.W.Henrion, et al, Wide Dynamic Range Direct Digital Accelerometer, *Tech.Digest of IEEE Solid-state Sensor and Actuator Workshop*, pp.153-157, Hilton Head Island, (1990)
10.Minhang Bao, et al, Analysis on Twin-mass Structure for a Piezoresistive Accelerometer, Sensors and Actuators A34, pp.101-107, (1992)
11.S.Timoshenko,*Vibration Problems in Engineering*, 4th Editon, John Wiley and Sons, Inc., pp.22, (1974)
12.James B. Starr, Squeeze-film Damping in Solid-state Accelerometers, *Tech.Digest of IEEE Solid-state Sensor and Actuator Workshop, pp.44-47*, Hilton Head Island, (1990)
13.Li Xinxin,et al, The Characteristics and Applications of Aqueous KOH maskless Etching to Silicon 3-D Sensing Structures, *Proc. Int. Conf. Electronic Components and Materials Sensors and Actuators*, pp.332-335 , Xi'an, China (1995)
14.Xingguo Xiong, et al, Balance-approach For Mechanical Properties Test of Micro Fabricated Structure, *proc. of SPIE conf. on Micromachining and Microfabrication 97*, to be published , Austin, USA, (1997)